Excitation functions of $(n,2n)$, (n,p), $(n,np+pn+d)$, and (n,α) reactions on isotopes of chromium

A. Fessler,[1,2] E. Wattecamps,[2] D. L. Smith,[2,3] and S. M. Qaim[1]
[1]*Institut für Nuklearchemie, Forschungszentrum Jülich GmbH, D-52425 Jülich, Germany*
[2]*Commission of the European Communities, Joint Research Centre, Institute for Reference Materials and Measurements, B-2440 Geel, Belgium*
[3]*Argonne National Laboratory, Technology Development Division, Argonne, Illinois 60439*
(Received 23 April 1998)

Excitation functions were measured for the $^{52}Cr(n,2n)^{51}Cr$, $^{52}Cr(n,p)^{52}V$, $^{53}Cr(n,p)^{53}V$, $^{53}Cr(n,np+pn+d)^{52}V$, $^{54}Cr(n,p)^{54}V$, $^{54}Cr(n,np+pn+d)^{53}V$, and $^{54}Cr(n,\alpha)^{51}Ti$ reactions from 9 to 21 MeV. Use was made of the activation technique in combination with high-resolution γ-ray spectrometry. Monoenergetic neutrons produced via the $^{2}H(d,n)^{3}He$ and $^{3}H(d,n)^{4}He$ reactions were used to irradiate samples of metallic chromium, $^{52}Cr_2O_3$, $^{53}Cr_2O_3$, and $^{54}Cr_2O_3$. The neutron fluence rates were determined via the $^{27}Al(n,p)^{27}Mg$, $^{27}Al(n,\alpha)^{24}Na$, $^{56}Fe(n,p)^{56}Mn$, and $^{93}Nb(n,2n)^{92m}Nb$ monitor reactions. Short-lived activities were investigated using a pneumatic sample transport system. Statistical model calculations taking into account preequilibrium effects were performed for all the reactions using a consistent set of model parameters. The experimental excitation functions helped appreciably to resolve the discrepancies in evaluated data files. Good agreement was found between our experimental data and the new model calculations.
[S0556-2813(98)07008-3]

PACS number(s): 24.10.−i, 24.60.Dr, 27.40.+z

I. INTRODUCTION

Studies of excitation functions of fast neutron-induced reactions are of considerable interest in testing nuclear models. However, extensive data exist only around 14 MeV. In the energy ranges 8–13 MeV and 15–20 MeV relatively few measurements have been done and the results are often inconsistent. Different cross section evaluations, mostly based on model calculations, differ frequently by a factor of 2–3. Since in the energy region up to 20 MeV many reaction channels are open [e.g., elastic and inelastic scattering, radiative capture, $(n,2n)$, (n,p), (n,α), (n,np), (n,d), $(n,n\alpha)$, etc.], different reaction mechanisms need to be considered (compound, precompound, and direct interactions). For nuclear reaction model calculations several computer codes, based mainly on compound-precompound mechanisms, are available but the parametrization is often uncertain. Therefore more experimental data are needed to test the model parametrizations. Of special interest are investigations on a series of isotopes of a particular target element or a particular mass region to develop such parameters in a systematic way and thus to improve the reliability of extrapolations based on these models. We chose to investigate the excitation functions of $(n,2n)$, (n,p), (n,np), and (n,α) reactions on ^{52}Cr, ^{53}Cr, and ^{54}Cr which lead to radioactive products and are thus measurable via the activation method. Special emphasis was given to those energy regions where no data existed. Apart from this fundamental interest, the activation data on chromium are important for practical applications in fusion reactor technology (e.g., estimation of activity level, hydrogen and helium gas production, nuclear heating, and radiation damage) since chromium is an important constituent of structural steel.

II. EXPERIMENT

A. Sample irradiations

High-purity metallic natural chromium samples (99.9%, 1 mm thick, supplied by Goodfellow Metals, Cambridge, England) were fabricated with a laser cutting technique into small disks (1.0 g, 1.3 cm in diameter). Samples of enriched $^{53}Cr_2O_3$ and $^{54}Cr_2O_3$, each containing 50 mg of chromium (supplied by CHEMOTRADE GmbH, Düsseldorf, Germany), were pressed into small pellets (1.0 cm in diameter) and covered with a thin Scotch tape. Some samples of $^{53}Cr_2O_3$ (50 mg each, borrowed from JAERI-Tokai-mura, Japan, originally supplied by Oak Ridge Laboratory) were not pressed but just wrapped in a small cartridge paper (1.0 cm×1.0 cm). Reference samples were thin metallic foils of aluminum, iron, and niobium (99.9%, 100–250 μm thick, 1.3 cm in diameter, supplied by Goodfellow Metals, Cambridge, England).

Three series of irradiations were carried out using different experimental facilities. At the variable-energy Compact Cyclotron CV 28 at Jülich, irradiations with quasimonoenergetic neutrons in the energy range of 9.3–12.3 MeV were performed using the $^{2}H(d,n)^{3}He$ reaction ($Q=3.269$ MeV) with a D_2 gas target. The details of the neutron source and the irradiation geometry are described in [1,2]. The natural chromium samples, each sandwiched between two aluminum and iron foils, were irradiated in the 0° direction relative to the incident deuteron beam at currents of approximately 4 μA. The distance between the sample and the back of the beam stop was 1.0 cm. For each chosen deuteron energy, one irradiation was done with a filled cell (gas in) and one with an empty cell (gas out), both of them in an identical geometry. The gas-out irradiations are needed to allow for a small correction due to the background neutrons stemming from interactions of the deuterons with structural materials (entrance window, beam stop, cell wall, etc.). At the highest

incident deuteron energy of 9.7 MeV the contribution of these background neutrons to the total activation was 5–10 %, depending on the reaction threshold of the investigated reaction. The irradiation time was 10 min for each sample and the beam current was always recorded with a charge integrator.

At the 7 MV Van de Graaff accelerator at Geel, irradiations with quasimonoenergetic neutrons in the energy range of 13.3–21.0 MeV were performed using the $^{3}H(d,n)^{4}He$ reaction ($Q=17.59$ MeV) with a solid-state Ti/T target (2.042 mg/cm^2 thick) on a silver backing (0.4 mm thick). Here two different irradiation geometries were used. One allowed the irradiation of several samples simultaneously at several angles. This is useful for long irradiations since due to the angular distribution of the $^{3}H(d,n)^{4}He$ reaction several samples can be irradiated with different neutron energies in one experiment. In an irradiation of 100 h, a total of seven sample stacks, each containing three chromium disks and one thick nickel pellet (1.4 cm in diameter, $\sim$5.0 g) sandwiched between five niobium reference foils, were fixed symmetrically to the ion beam direction in an aluminum sample holder ring, as described in [3]. The second and third chromium disks as well as the nickel pellet were part of another experiment and thus are just given for completeness but are not considered here any further. The sample holder ring was adjusted with its center above the nominal source position. Nominal angles were 0°, 30°, 60°, and 105°, and the distance between the front of each sample stack and the target was 3 cm. In addition to this long irradiation, some short irradiations (10 min) were performed with the samples previously used at Jülich. Here only one sample at a time was irradiated at angles of 0°, 60°, and 110°.

The third irradiation geometry, also at Geel, used a pneumatic sample transport system of 20 m length, especially designed for measurements on short-lived isotopes [4]. The samples were placed in a small container which was pushed with compressed air through a plastic tube to the target, stopped at a distance of 1 cm in the 0° direction relative to the deuterium beam, and sucked back by a vacuum pump after completion of the irradiation. Details about the pneumatic sample transport system are given elsewhere [5]. With this system, the samples (mainly the enriched isotopes) were sandwiched between two aluminum foils and irradiated for short periods (3–10 min). In order to allow cross-checks with the other irradiation setup some natural chromium disks were also irradiated. During the irradiations at Geel the beam current was between 5 and 15 μA. The source intensity was continuosly monitored by counting the neutrons with a Bonner sphere or with a long counter operated in the multichannel-scaling acquisition mode.

B. Mean neutron energies and flux densities

The average neutron energy effective at each sample in the DD neutron field was calculated using the Monte Carlo program NEUT-HAV [6], an improved version of the code NEUT [7]. It takes into account the energy loss, energy spread, and angular straggling of the deuterons in the entrance window of the gas cell, the neutron production within the volume of the gas cell, the angular distribution of the $^{2}H(d,n)^{3}He$ reaction, the breakup of the deuterons in the D_2 gas according to the results from [8], and the activation geometry. For the DT neutron field the NEUT-HAV code was slightly modified by implementing the geometry of the Ti/T target as well as the angular distribution of the $^{3}H(d,n)^{4}He$ source reaction [9].

The neutron flux densities were determined via the $^{27}Al(n,p)^{27}Mg$, $^{27}Al(n,\alpha)^{24}Na$, $^{56}Fe(n,p)^{56}Mn$, and $^{93}Nb(n,2n)^{92m}Nb$ activation cross sections by determining the activities of the reaction products in the respective monitor foils sandwiching the chromium samples. These activities were determined via γ-ray spectrometry in the same way as the activities induced in the chromium samples (see the following section). The activities were corrected for contributions from background neutrons. For the experiments with the gas target, the gas-in–gas-out corrected activity was calculated first as described in [10]. Then the corrections for the breakup neutrons were determined from the neutron spectra calculated with the NEUT-HAV program, using the cross sections taken from the IRDF-90.2 computer file [11]. The ratio of the activity induced by breakup neutrons to the activity induced by monoenergetic neutrons was calculated and used for the corrections (see also Ref. [8]). In order to estimate the contribution of background neutrons in the DT neutron field, the neutron spectra were determined experimentally by time-of-flight (TOF) measurements. For these measurements the Van de Graaff accelerator was operated in the pulsed mode and the neutrons were detected with an NE-213 liquid scintillation detector which was placed 2.69 m behind the target at variable angles. The detector efficiency was calculated with the Monte Carlo code NEFF7, an updated version of the NEFF4 code [12]. The corrections for the low-energy neutrons were then applied in a similar way as was done for the DD breakup neutrons. Finally, the average fluence rates at the sample positions were determined by appropriately averaging the corrected activities and using the cross sections from the IRDF-90.2 computer file (see above). The decay data of the products were taken from the literature [13] and are given in Table I. In cases where more than one reference reaction was used to determine the neutron fluence rate, the individual results were averaged. Generally, the agreement between the individual results was within 5% [5]. In the experiments on the short-lived reaction products, in order to save time, the two aluminum monitor foils were counted simultaneously with the sample. Here the activities of the aluminum foils yield directly the average neutron fluence rate effective for the sample.

C. Measurement of radioactivity

The radioactivity of each activation product investigated was determined via standard γ-ray spectrometry. For this purpose three lead-shielded (5 cm thick) HPGe detectors, two at Geel (28% and 45% relative efficiency) and one at Jülich (15% relative efficiency) were used. The detectors at Geel were connected via two analog-to-digital converters (ADC's) to a PC plug-in MCA card and the data acquisition was controlled with the software TMCA (supplied by TARGET GmbH, Solingen, Germany). The detector at Jülich was connected to a 92$\times$ Spectrum Master and controlled with the software GAMMAVISION (supplied by EG&G Ortec, Oak Ridge). The counting was done in the following way. The

TABLE I. Decay data of measured reaction products, taken from *Table of Isotopes* [13]. The Q values were calculated from atomic masses given in [28].

Nuclear reaction	Q value (MeV)	Half-life of the product	Decay mode (% branching)	γ-ray energy (keV)	γ-ray abundance (%)
Investigated reactions					
^{52}Cr$(n,2n)^{51}$Cr	−12.0395	27.70 d	EC [a] (100)	320.1	9.86
^{52}Cr$(n,p)^{52}$V	−3.1931	3.75 min	β^- (100)	1434.1	100.0
^{53}Cr$(n,d)^{52}$V	−8.9077				
^{53}Cr$(n,np)^{52}$V	−11.3444				
^{53}Cr$(n,p)^{53}$V	−2.6537	92.3 s[b]	β^- (100)	1006.0	89.6
^{54}Cr$(n,d)^{53}$V	−8.9077				
^{54}Cr$(n,np)^{53}$V	−11.1323				
^{54}Cr$(n,p)^{54}$V	−6.2593	49.8 s	β^- (100)	834.8	97.1
				989.0	80.1
^{54}Cr$(n,\alpha)^{51}$Ti	−1.5551	5.76 min	β^- (100)	320.1	93.4
Monitor reactions					
^{27}Al$(n,\alpha)^{24}$Na	−3.1328	14.96 h	β^- (100)	1368.6	100.0
^{27}Al$(n,p)^{27}$Mg	−1.8280	9.46 min	β^- (100)	843.8	71.8
				1014.4	28.0
^{56}Fe$(n,p)^{56}$Mn	−2.9131	2.58 h	β^- (100)	846.8	98.9
				1810.7	27.2
^{93}Nb$(n,2n)^{92m}$Nb	−8.9667	10.15 d	EC ($\geqslant$99), β^+ ($\leqslant$1)	934.4	99.1

[a]Electron capture.
[b]Taken from [14].

samples were placed either directly on the detector or at a distance of 0.5 cm from the end cap of the detector. Generally the measuring time for the short-lived isotopes was two or three times the half-life and a correction was applied for the decay during the measurement. The decay data were taken from Ref. [13] (see Table I). In one case, namely, the nuclide ^{53}V, the half-life was taken from a recent measurement [14]. When the activity of the product was high enough a decay curve was recorded and the initial activity was determined by least-squares fitting to the measured counts as a function of time using the half-life given in the literature. The peak area analysis was done with the PC program GAMMA-W V17.07 [15]. The photopeak efficiencies of the detectors were determined using calibrated standard sources, obtained from PTB, Braunschweig, Germany, and DAMRI, Gif-sur-Yvette, France. The measured calibration points were fitted with an analytical function described in [16]. The total efficiency curves were determined [17] to correct for coincidence losses, which were estimated from the decay schemes [13].

D. Calculation of the cross section

The count rates were corrected for coincidence losses as well as for γ-ray abundance, γ-ray self-absorption, efficiency of the detector, and differences between the geometries of the samples and the calibration sources. Corrections for neutron flux fluctuations during the irradiations were also taken into account using the multichannel-scaling spectra recorded with the Bonner sphere or the long counter. The procedure is explained in [18]. The contributions from the background neutrons were estimated as described for the monitor reactions (see Sec. II B). But instead of using the evaluated cross sections, we used our preliminary data or a model calculation (see the following section). This approach seems to be justified since our new measurements improve the knowledge of most of the investigated reactions for which the evaluations show big discrepancies. For the experiments using the pneumatic transport system, neutron multiple scattering corrections were done using the code CYSCT3 [19] (for details see [5]). Since these scattering corrections are quite small (less than 5%), and are expected to be even smaller for the other two irradiation geometries, we did not take multiple scattering into account for these latter two geometries. After applying all the corrections, the cross sections were calculated using the usual activation formula. The uncertainties of the measured cross sections amount to 5–10 %. They were obtained by taking the square root of the quadratic sum of all the individual uncertainties.

III. NUCLEAR MODEL CALCULATIONS

The cross section calculations were performed by means of the code STAPRE-H [20,21], a modified version of STAPRE [22], which uses the Hauser-Feshbach formula and the exciton or geometry-dependent hybrid model (GDH) for the first-chance preequilibrium (PE) emission of particles. Both the statistical and the preequilibrium models require optical potentials to calculate transmission coefficients and inverse reaction cross sections. Before using an optical potential to generate transmission coefficients and reaction cross sections, the potentials were checked by comparing their predictions of particle emission, nonelastic, and total cross sections with experimental data, where available. The calculation of the transmission coefficients was done with the code SCAT

TABLE II. Level density parameter a, backshift Δ, and number of discrete levels N up to excitation energy E_x used in STAPRE-H calculations. a and Δ were taken from [30]. In those cases where a was slightly modified, the value from [30] is given in brackets.

Nuclide	a [MeV^{-1}]	Δ [MeV]	N	E_x [MeV]
^{47}Ca	5.55	0.25	17	4.103
^{48}Sc	6.00	−1.20	30	2.891
^{49}Sc	5.60	0.48	18	4.493
^{50}Sc	6.20	0.10	9	2.614
^{48}Ti	5.55	−0.25	21	3.852
^{49}Ti	6.25	−0.50	15	2.720
^{50}Ti	5.40	0.77	11	2.084
^{51}Ti	5.55	−0.52	15	3.237
^{53}Ti	5.70[a]	0.00[a]	1	0.000
^{51}V	5.78	−0.88	25	3.454
^{52}V	6.10	−1.58	24	2.428
^{53}V	5.80 (5.60)	−1.42	11	2.084
^{54}V	6.35 (6.15)	−2.05	15	1.215
^{51}Cr	5.30 (5.70)	−1.40	34	3.207
^{52}Cr	5.67 (5.80)	0.60	24	4.837
^{53}Cr	5.60	−1.07	17	2.827
^{54}Cr	5.60 (5.70)	−0.12	25	4.254
^{55}Cr	6.10	−1.20	16	2.390

[a]Estimated, since the level scheme is unknown.

[23] which is implemented as a subroutine. The neutron transmission coefficients were calculated with the optical model potential of Ferrer *et al.* [24], modified by Uhl *et al.* [25]. Proton and alpha transmission coefficients were calculated with the optical potential of Arthur and Young [26] and Avrigeanu *et al.* [27], respectively. The nuclear masses used were taken from the atomic mass evaluation done by Audi and Wapstra [28]. The discrete levels, including information about energy, spin, parity, and γ-ray branching, were taken from [13]. Levels up to excitation energies of $\sim$4 MeV were included where the level information seemed to be complete. The level density above the discrete levels was calculated by the backshifted Fermi-gas model [29]. The level density parameter and the backshift were taken from the compilation of Avrigeanu *et al.* [30]. In some cases they were slightly modified in order to fit better the experimentally determined excitation functions [i.e., a decrease of the level density parameter for ^{51}Cr from 5.70 to 5.30 resulted in a decrease of the ^{52}Cr$(n,2n)^{51}$Cr excitation function of 3%]. They are given in Table II. The preequilibrium emission was calculated with both models. In the exciton model we chose the energy and mass dependence of the effective matrix element for internal transitions as $|M|^2 = F_M \times A^{-3} E^{-1}$, with F_M calculated according to [31]. The sensitivity of the cross section to this parameter was tested by modifying its value by $\pm 20\%$. In the GDH model the preequilibrium emission was calculated with a version of the code HYBRID [32] (implemented as a subroutine) including angular momentum, parity conservation, and alpha emission. A so-called composite single-particle state density, based on the Fermi-gas model, was chosen according to [33]. Direct reaction contributions were accounted for in the case of inelastic neutron scattering on low-lying levels. They were estimated from distorted-wave Born approximation (DWBA) calculations [25,34] to be on the order of 3–8 % of the total cross section.

IV. RESULTS AND DISCUSSION

A. Excitation functions

The cross sections are given in Tables III and IV and are plotted, together with the data available in the literature [18,35–68], as a function of neutron energy in Figs. 1–7. The results of some major evaluations, as well as the STAPRE-H calculations, are also shown. The STAPRE-H plots describe the calculations with the exciton model, using a slightly modified F_M parameter. Some remarks on the individual reactions are given below.

The excitation function of the ^{52}Cr$(n,p)^{52}$V reaction is shown in Fig. 1. Our data provide, together with the recent measurement of Mannhart *et al.* [35], the first cross sections in the so-called ''gap region'' between 9 and 14 MeV. Our two lowest-energy points match the data of Smith and Meadows [36] at the threshold region and are also in good agreement with those of Mannhart *et al.* but at higher energies the latter are somewhat higher (consistent with JEF-2.2 evaluation and the STAPRE-H calculation). Our data above 14 MeV, measured with enriched as well as natural sample material, are consistent. The two other existing data sets in this energy region have the same shape of the excitation function but are either much higher [37] or lower [38] than our data. At 14 MeV the data of Mannhart *et al.* as well as of Viennot *et al.*

TABLE III. Cross sections determined using natural sample material.

Neutron energy [MeV]	Cross section [mb] ^{52}Cr$(n,2n)^{51}$Cr	^{52}Cr$(n,p)^{52}$V	^{53}Cr$(n,p)^{53}$V
9.31±0.20		50.8±3.5	
10.33±0.22		55.1±3.6	
11.57±0.24		65.3±3.9	28.3±6.0
12.27±0.26		70.7±4.4	36.4±5.7
13.71±0.25		88.2±5.6	48.9±6.0
14.25±0.20	330.3±17.0		
15.01±0.25		82.9±4.1	46.4±4.3
15.95±0.25		74.7±3.6	42.3±3.5
16.02±0.25		79.6±3.9	48.4±2.9
16.99±0.20		65.8±4.3	45.8±4.3
17.20±0.25	591.0±29.1		
17.54±0.30		59.3±3.7	
17.73±0.25		58.3±4.1	45.7±3.4
17.80±0.30		58.9±3.2	40.5±5.2
18.73±0.35		45.5±2.7	30.5±2.8
18.80±0.30	621.9±31.3		
19.04±0.25		46.6±3.1	35.2±2.8
19.40±0.32	637.4±33.2		
19.70±0.40		34.2±1.7	19.7±2.2
20.24±0.25		28.8±2.1	16.8±1.3
21.07±0.50		27.1±2.6	15.4±2.3

[39] are confirmed. The data of Ikeda *et al.* [18] and Kawade *et al.* [40] around 14 MeV are 10% lower than all the others. Many single data points around 14 MeV have not been included in the figure for reasons of simplicity and clarity. They all lie between 75 and 100 mb (see Refs. [41–47]).

The ^{52}Cr$(n,2n)^{51}$Cr cross sections, shown in Fig. 2, split above 16 MeV into two groups. The data of Liskien *et al.* [48] represent a higher trend while those of Ghorai *et al.* [38] and Bormann *et al.* [49] show a lower trend in the excitation function. The evaluations also split in these two groups, ENDF/B-VI relying on Liskien *et al.* and JENDL-3.2 on Ghorai *et al.* and Bormann *et al.* Our data agree well with the data of Liskien *et al.* and the new data of Mannhart *et al.* at 14 MeV [35]. Keeping in mind that the data of Ghorai *et al.* also for the (n,p) reaction are systematically lower by 20–30 %, it is seen that the higher trend in the excitation function is clearly validated. For both the (n,p) and $(n,2n)$ reactions on ^{52}Cr our model calculation is in very good agreement with the new data over the whole energy range. The small overestimation of the $(n,2n)$ cross section ($\sim$8%) could not be solved by a parameter adjustment since each variation which decreased this cross section simultaneously increased the (n,p) value.

Figure 3 shows the excitation function of the ^{53}Cr$(n,p)^{53}$V reaction. We report the first measurements in the ''gap region'' between 9 and 14 MeV and above 15 MeV. Our data around 14 MeV are consistent with the average value of the literature data. The discrepancies in the three given evaluations are resolved by a clear support of the ENDF/B-VI through the new experimental data. The model calculation follows the trend of the experimental data up to 19 MeV; at higher energies it is 20% higher than the experimental data.

The situation for the ^{53}Cr$(n,pn+np+d)^{52}$Cr reaction is shown in Fig. 4. We report again the first experimental data above 15 MeV. They agree fairly well with the evaluations and the model calculation (±20%). The calculated individual contributions of the (n,pn), (n,np), and (n,d) reac-

TABLE IV. Cross sections determined using enriched sample material. The (n,pn) reaction includes contributions from the (n,np) and (n,d) reactions.

Neutron energy [MeV]	Cross section [mb] ^{52}Cr$(n,p)^{52}$V	^{53}Cr$(n,p)^{53}$V	^{53}Cr$(n,pn)^{52}$V	^{54}Cr$(n,p)^{54}$V	^{54}Cr$(n,pn)^{53}$V	^{54}Cr$(n,\alpha)^{51}$Ti
16.02 ± 0.25	76.0 ± 3.8	49.2 ± 3.6	26.1 ± 2.1	22.4 ± 1.7	6.5 ± 0.6	14.1 ± 1.2
16.99 ± 0.20	61.7 ± 4.1	43.9 ± 5.6	55.3 ± 4.2	26.3 ± 2.0	15.0 ± 1.6	14.3 ± 1.4
17.73 ± 0.25	57.4 ± 3.2	41.2 ± 5.0	70.9 ± 5.0	27.1 ± 2.1	22.5 ± 2.3	14.3 ± 1.3
19.04 ± 0.25	40.5 ± 2.7	28.0 ± 3.1	77.7 ± 5.5	21.1 ± 1.8	35.3 ± 2.5	10.3 ± 0.9
20.24 ± 0.25	28.3 ± 2.6	20.0 ± 2.1	78.1 ± 5.8	14.3 ± 1.5	32.5 ± 3.0	6.1 ± 0.7

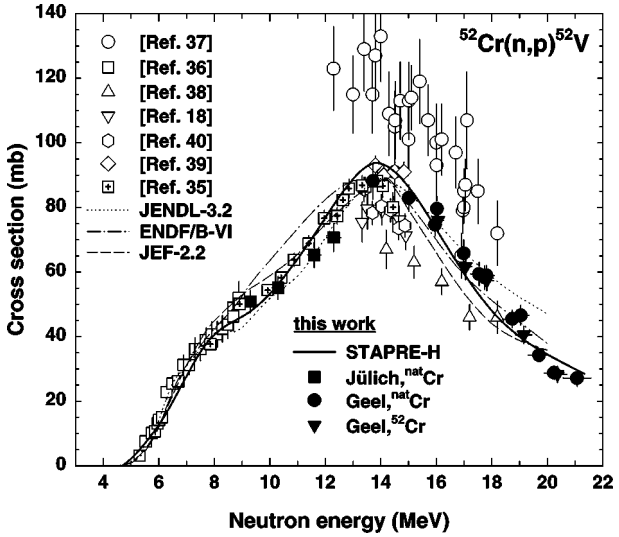

FIG. 1. Excitation function of the ^{52}Cr$(n,p)^{52}$V reaction. Besides our results the literature data are also shown. Some more results in the 14 MeV region given in Refs. [41–47] are not shown.

tions to the formation of ^{52}V are also indicated in Fig. 4.

The excitation functions of the ^{54}Cr$(n,p)^{54}$V, ^{54}Cr$(n,pn+np+d)^{53}$V, and ^{54}Cr$(n,\alpha)^{51}$Ti reactions are shown in Figs. 5–7. All of them have been hitherto poorly investigated due to the low natural abundance of ^{54}Cr. Our data represent the first values above 14 MeV, and they agree fairly well with the model calculation. The three given evaluations are contradictory for all the three reactions. The best reproduction of the experimental data is given by JENDL-3.2. Of particular interest concerning the model calculation is the fact that all three reactions on ^{54}Cr, involving emission of different types of particles, are described well by our calculation, using one parameter set.

B. Effect of preequilibrium models

The influence of the chosen preequilibrium model on the calculated excitation functions was investigated, and this is

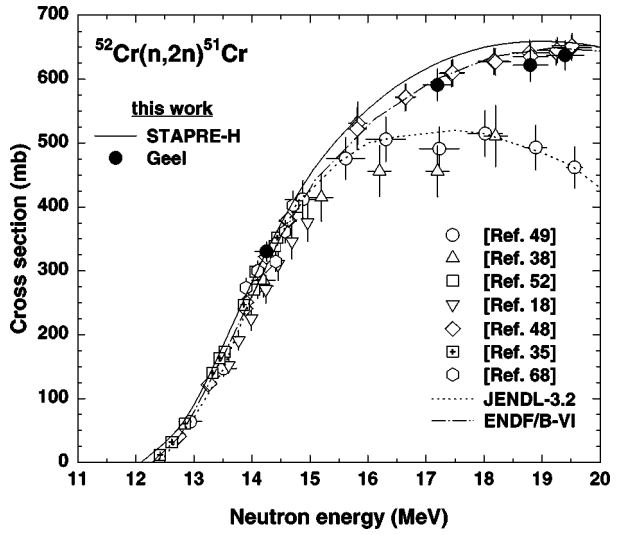

FIG. 2. Excitation function of the ^{52}Cr$(n,2n)^{51}$Cr reaction. Besides our results the literature data are also shown. Some more results in the 14 MeV region given in Refs. [53–61] are not shown.

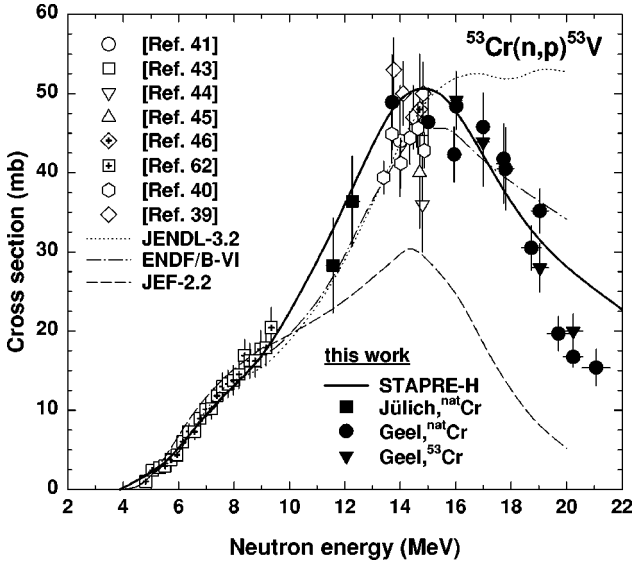

FIG. 3. Excitation function of the ^{53}Cr$(n,p)^{53}$V reaction.

illustrated in Figs. 8 and 9. The GDH model (bold lines in the figures) and the exciton model with standard F_M parameter (calculated according to [31], dotted lines in the figures) lead to quite similar results. The decrease of F_M increases the preequilibrium (PE) fraction and makes the first-chance emission spectrum harder. This reduces the second chance emission. This effect can be seen for the reactions on ^{52}Cr (see Fig. 8). The reduction of F_M increases the ^{52}Cr$(n,n')^{52}$Cr cross section at the cost of the ^{52}Cr$(n,2n)^{51}$Cr cross section, and the ^{52}Cr$(n,p)^{52}$V cross section increases at the cost of the ^{52}Cr$(n,pn)^{51}$V cross section. The (n,p) reaction is best reproduced with a slightly increased F_M value whereas the $(n,2n)$ reaction data are fitted better with a decreased F_M value. Similar results for the (n,p) and $(n,pn+np+d)$ reactions on ^{53,54}Cr are shown in Fig. 9. The influence of F_M on the (n,p) reaction on ^{53}Cr and ^{54}Cr is much stronger than in the case of the ^{52}Cr(n,p) reaction whereas the $(n,pn+np+d)$ reactions

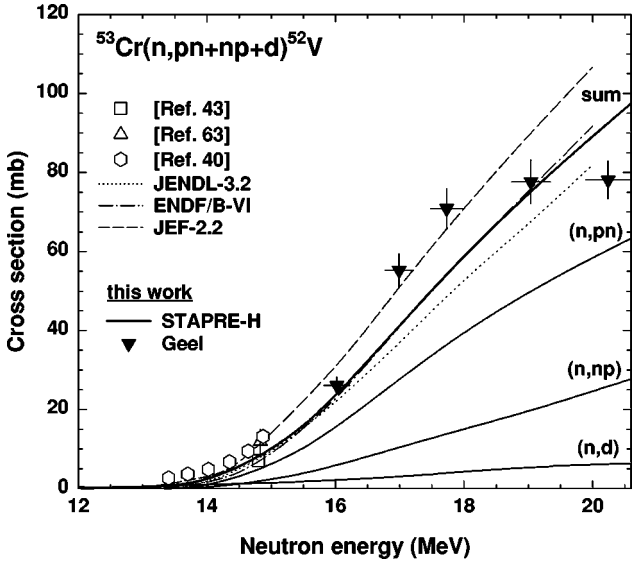

FIG. 4. Excitation function of the ^{53}Cr$(n,pn+np+d)^{52}$V process.

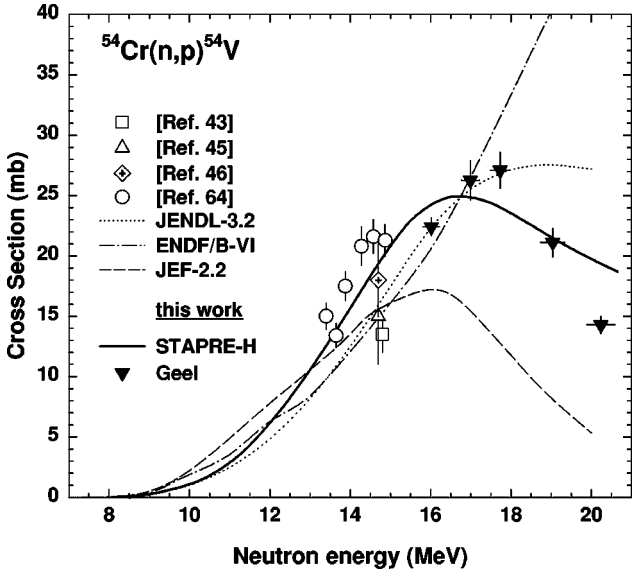

FIG. 5. Excitation function of the ^{54}Cr$(n,p)^{54}$V reaction.

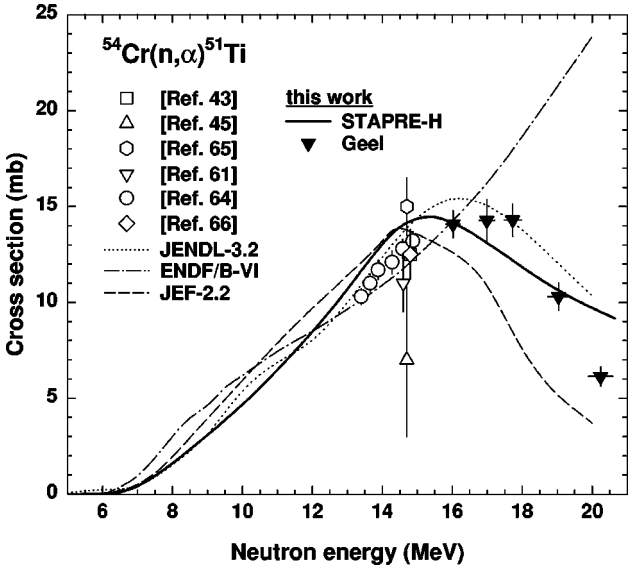

FIG. 7. Excitation function of the ^{54}Cr$(n,\alpha)^{51}$Ti reaction.

are almost independent of F_M. It seems that opposite effects on the (n,pn) and (n,np) reactions compensate each other.

C. Systematics of excitation functions

The isotope effect for the (n,p) reaction, stated by several authors [46,50,51], could be clearly demonstrated here. Figure 10 shows the result of the present experiment together with the STAPRE-H calculations for the (n,p) and $(n,pn+np+d)$ reactions on ^{50}Cr, ^{52}Cr, ^{53}Cr, and ^{54}Cr. For the ^{50}Cr(n,p) and ^{52}Cr$(n,pn+np+d)$ reactions only the calculation is shown since these reactions lead to stable products and thus are not measurable with the activation method. With increasing target mass number the maximum cross section for the (n,p) reaction on adjacent isotopes decreases by about a factor of 2 [estimating a maximum cross section for the ^{51}Cr(n,p) reaction of about 200 mb]. The maximum position is shifted from 12.5 MeV for ^{50}Cr to 16.5 MeV for ^{54}Cr. The threshold of the reaction increases with the increasing mass number, the odd-even isotopes having a somewhat smaller threshold than the even-even ones, an effect attributable to the pairing energy. The isotope effect decreases with increasing neutron energy since the Q-value effect becomes less important. The same trend can be stated for the $(n,pn+np+d)$ reactions. In no previous study has such a trend been reported explicitly.

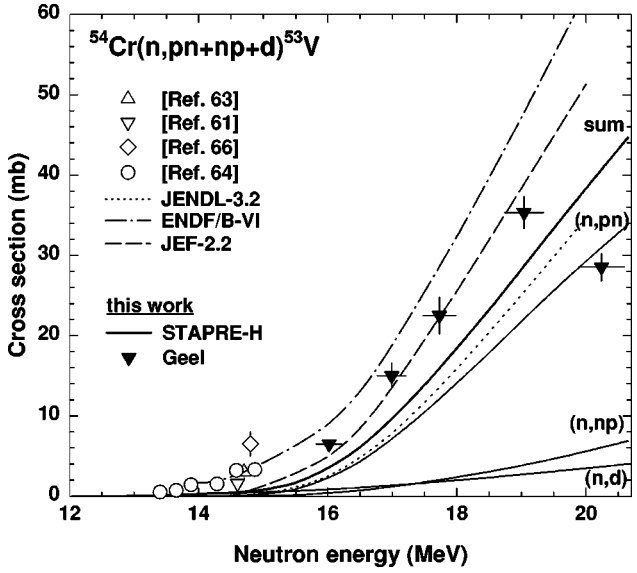

FIG. 6. Excitation function of the ^{54}Cr$(n,pn+np+d)^{53}$V process.

V. SUMMARY AND CONCLUSIONS

Data were measured for the first time for the ^{52}Cr$(n,p)^{52}$V and ^{53}Cr$(n,p)^{53}$V reactions in the ''gap region'' between 9 and 14 MeV. Beyond 14 MeV substantial

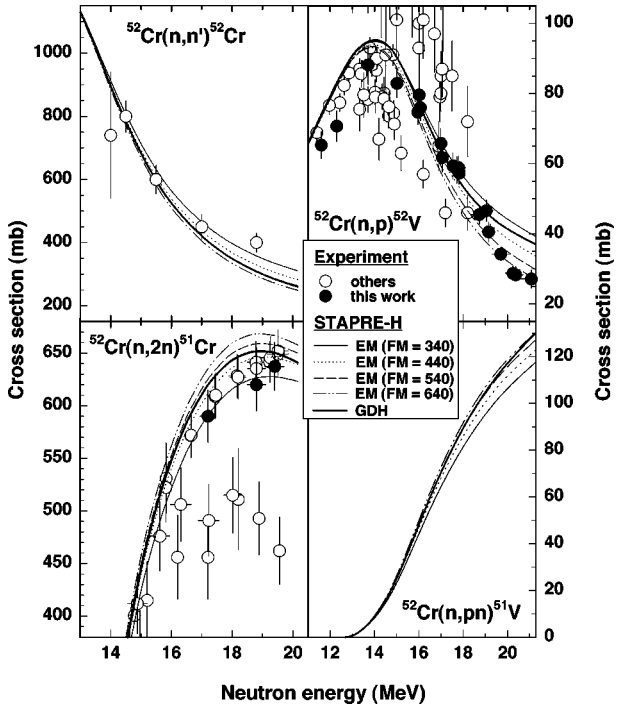

FIG. 8. Influence of the F_M parameter in the exciton model on the excitation functions of different reactions on ^{52}Cr, and comparison with the results of the GDH model.

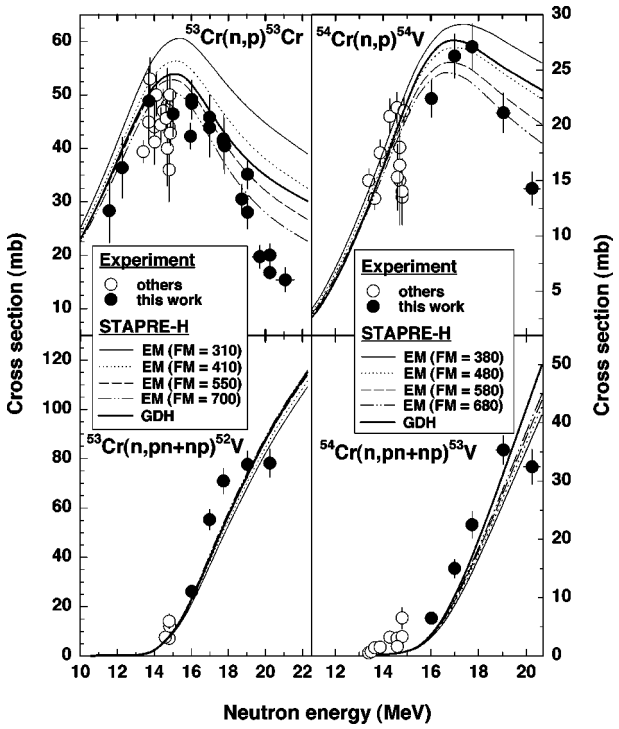

FIG. 9. Influence of the F_M parameter in the exciton model on the excitation functions of different reactions on ^{53}Cr and ^{54}Cr, and comparison with the GDH model.

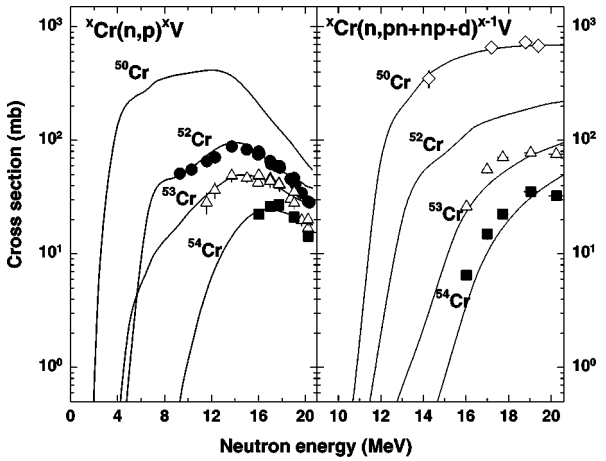

FIG. 10. Systematics of excitation functions of (n,p) and $(n,pn+np+d)$ reactions on Cr isotopes. The symbols represent the experimental data points of this work, the solid lines the STAPRE-H calculations. The data points for the ^{50}Cr$(n,pn+np+d)^{49}$V process were taken from a recent measurement [67].

new information was obtained for several reactions. In the case of ^{52}Cr$(n,2n)^{51}$Cr and ^{54}Cr$(n,\alpha)^{51}$Ti reactions the database was strengthened. For all the studied reactions on the Cr isotopes, especially for the ^{53}Cr$(n,p)^{53}$V, ^{54}Cr$(n,p)^{54}$V, and ^{54}Cr$(n,\alpha)^{51}$Ti reactions, where large discrepancies existed in the major evaluations, the present data contribute appreciably to solving those discrepancies. Furthermore, for the (n,p) and (n,pn) reactions, some systematic trends in the excitation functions, ascribed to the Q values of the reactions, could be observed.

From the results presented above it is concluded that the measurement of cross sections on a series of Cr isotopes has been very helpful in developing a consistent parameter set for nuclear model calculations. All the investigated reactions are described relatively well by the STAPRE-H calculations.

ACKNOWLEDGMENTS

We thank the crews of the Van de Graaff accelerator (Geel) and the Compact Cyclotron (Jülich) CV 28 for irradiations and S. Spellerberg for experimental assistance. Some useful discussions with Dr. A. J. M. Plompen and Dr. S. Sudár are acknowledged. Dr. J. W. Meadows is thanked for performing the multiple scattering corrections. A.F. is grateful to the Commission of the European Communities for support.

[1] S. M. Qaim, R. Wölfle, M. M. Rahman, and H. Ollig, Nucl. Sci. Eng. **88**, 143 (1984).
[2] Á. Grallert, J. Csikai, S. M. Qaim, and J. Knieper, Nucl. Instrum. Methods Phys. Res. A **334**, 154 (1993).
[3] A. Pavlik, G. Winkler, H. Vonach, A. Paulsen, and H. Liskien, J. Phys. G **8**, 1283 (1982).
[4] A. Fessler, Y. Ikeda, J. W. Meadows, S. M. Qaim, D. L. Smith, and E. Wattecamps, in *Proceedings of the International Conference on Nuclear Data for Science and Technology*, Trieste, 1997, edited by G. Reffo, A. Ventura, and C. Grandi (Italian Physical Society, Bologna, Italy, 1997), p. 399.
[5] A. Fessler, ''Activation Cross Sections and Isomeric Cross Section Ratios in Neutron Induced Reactions on Cr-, Fe- and Ni-Isotopes in the Energy Range 9 to 21 MeV,'' Forschungszentrum Jülich GmbH Report No. Jül-3502, 1998.
[6] I.-G. Birn, ''Calculation of the Mean Energy and the Energy Spread of Neutrons Produced by the $D(d,n)^3$He Reaction in a Gas Target,'' CEC-JRC, IRMM, Geel, Internal Report No. GE/R/VG/85/94, 1994.
[7] I.-G. Birn, ''NEUT-Ein Programm zur Berechnung von Neutronenspektren erzeugt durch die $D(d,n)^3$He-Reaktion in einem Gastarget am Zyklotron,'' KFA-Jülich, Internal Report No. INC-IB-1/92, 1992.
[8] S. Cabral, G. Börker, H. Klein, and W. Mannhart, Nucl. Sci. Eng. **106**, 308 (1990).
[9] H. Liskien and A. Paulsen, Nucl. Data Tables **11**, 569 (1973).
[10] I.-G. Birn and S. M. Qaim, Nucl. Sci. Eng. **116**, 125 (1994).
[11] N. P. Kocherov and P. K. McLaughlin, International Reactor Dosimetry File, Report No. IAEA-NDS-141, IAEA, Vienna, 1993.
[12] G. Dietze and H. Klein, ''NRESP4 and NEFF4—Monte Carlo codes for the calculation of neutron response functions and detection efficiencies for NE-213 scintillation detectors,'' Report No. PTB-ND-22, PTB, Braunschweig, Germany, 1982.
[13] R. B. Firestone, *Table of Isotopes*, 8th ed., edited by V. S. Shirley (Wiley, New York, 1996), Vol. 1.
[14] D. L. Smith and A. Fessler, Radiochim. Acta **79**, 1 (1997).
[15] W. Westmeier and J. van Arle, Nucl. Instrum. Methods Phys. Res. A **268**, 439 (1990).
[16] B. Jäckel, W. Westmeier, and P. Patzelt, Nucl. Instrum. Methods Phys. Res. A **261**, 543 (1987).

[17] K. Debertin and R. G. Helmer, *Gamma and X-Ray Spectrometry with Semiconductor Detectors* (North-Holland, Amsterdam, 1988).
[18] Y. Ikeda, C. Konno, K. Oishi, T. Nakamura, H. Miyade, K. Kawade, H. Yamamoto, and T. Katoh, Report No. JAERI 1312, edited by T. Fuketa, JAERI Tokai-mura, Naka-gun, Ibaraki-ken, Japan, 1988).
[19] D. L. Smith and J. W. Meadows, Report No. ANL/NDM-37, Argonne National Laboratory, 1977.
[20] M. Avrigeanu, M. Ivascu, and V. Avrigeanu, ''STAPRE-H—A Computer Code for Particle Induced Activation Cross Sections and Related Quantities,'' Report No. NP-63-1987, IPNE, Bucharest, Romania, 1987.
[21] M. Avrigeanu and V. Avrigeanu, ''Recent Improvements of the STAPRE-H Preequilibrium and Statistical Model Code,'' Report No. NP-86-1995, IPNE, Bucharest, Romania, 1995.
[22] M. Uhl and B. Strohmaier, ''Computer Code for Particle Induced Activation Cross Section and Related Quantities,'' IRK Report No. 76/01; also addenda to this report, Vienna, 1976.
[23] O. Bersillon, Report No. CEA-N-2227, CE Bruyeres-le Chatel, France, 1981.
[24] J. C. Ferrer, J. D. Carlson, and J. Rapaport, Nucl. Phys. **A275**, 325 (1977).
[25] M. Uhl, H. Gruppelaar, H. A. J. van der Kamp, J. Kopecki, and D. Nierob, in *Proceedings of the International Conference on Nuclear Data for Science and Technology*, Jülich, 1991, edited by S. M. Qaim (Springer Verlag, Berlin, 1992), p. 924.
[26] E. D. Arthur and P. G. Young, Report No. LA-8626-MS (ENDF-304), Los Alamos National Laboratory, 1980.
[27] V. Avrigeaunu, P. E. Hodgson, and M. Avrigeanu, Phys. Rev. C **49**, 2136 (1994).
[28] G. Audi and A. H. Wapstra, Nucl. Phys. **A595**, 409 (1995).
[29] W. Dilg, W. Schantl, H. Vonach, and M. Uhl, Nucl. Phys. **A217**, 269 (1973).
[30] M. Avrigeanu, A. Harangozo, and V. Avrigeanu, ''Surface effects in Feshbach-Kerman-Koonin analysis of (n,n') and (n,p) reactions at 7 to 26 MeV,'' Report No. NP-85-1995, IPNE, Bucharest, Romania, 1995.
[31] B. Strohmaier, Report No. INDC(AUS)-7/G, IAEA, Vienna, Austria, 1982.
[32] M. Blann, Report No. COO-3494-10, Rochester University, Rochester, U.K., 1973.
[33] M. Avrigeanu and V. Avrigeanu, J. Phys. G **20**, 613 (1994).
[34] M. Avrigeanu, M. Ivascu, and V. Avrigeanu, Z. Phys. A **335**, 299 (1990).
[35] W. Mannhart, D. Schmidt, and D. L. Smith, in *Proceedings of the International Conference on Nuclear Data for Science and Technology*, Trieste, 1997, edited by G. Reffo, A. Ventura, and C. Grandi (Italian Physical Society, Bologna, Italy, 1997), p. 505.
[36] D. L. Smith and J. W. Meadows, Nucl. Sci. Eng. **76**, 43 (1980).
[37] B. D. Kern, W. E. Thompson, and J. Ferguson, Nucl. Phys. **10**, 226 (1959).
[38] S. K. Ghorai, J. R. Williams, and W. L. Aford, J. Phys. G **13**, 405 (1987).
[39] M. Viennot, M. Berrada, G. Paic, and S. Joly, Nucl. Sci. Eng. **108**, 298 (1991).
[40] K. Kawade, H. Yamamoto, T. Yamada, T. Katoh, T. Iida, and A. Takahashi, Report No. JAERI-M-90-171, NEANDC(J)-154/U, INDC (JPN)-140/L, JAERI, Tokai-mura, Naka-jun, Ibaraki-ken, Japan, 1990.
[41] D. Allan, Nucl. Phys. **24**, 274 (1961).
[42] B. Mitra and A. M. Ghose, Nucl. Phys. **83**, 157 (1966).
[43] L. Husain and P. K. Kuroda, J. Inorg. Nucl. Chem. **29**, 2665 (1967).
[44] R. Prasad and D. C. Sarkar, Nuovo Cimento **3**, 467 (1971).
[45] P. Holmberg, R. Rieppo, J. K. Keinänen, and M. Valkonen, J. Inorg. Nucl. Chem. **36**, 715 (1974).
[46] N. I. Molla and S. M. Qaim, Nucl. Phys. **A283**, 269 (1977).
[47] B. M. Bahal and R. Pepelnik, Report No. GKSS 85/E/11, Forschungszentrum Geesthacht GmbH, Geesthacht, Germany, 1984.
[48] H. Liskien, M. Uhl, M. Wagner, and G. Winkler, Ann. Nucl. Energy **16**, 563 (1989).
[49] M. Bormann, A. Behrend, I. Riehle, and O. Vogel, Nucl. Phys. **A115**, 309 (1968).
[50] N. I. Molla, S. M. Qaim, and H. Kalka, Phys. Rev. C **45**, 3002 (1992).
[51] R. Dóczi, V. Semkova, A. D. Majdeddin, Cs. Buczko, and J. Csikai, Report No. INDC(HUN-032), IAEA, Vienna, Austria, 1997.
[52] M. Wagner, G. Winkler, H. Vonach, Cs. Buczko, and J. Csikai, Ann. Nucl. Energy **16**, 623 (1989).
[53] R. Wenusch and H. Vonach, Aut. Österr. Akad. Wiss., Math-Naturwiss. Kl. **99**, 1 (1962).
[54] G. N. Maslov, F. Nasyrov, and N. F. Pashkin, Report YK-9, Obninsk reports, Obninsk, USSR (1972).
[55] S. M. Qaim, Nucl. Phys. **A185**, 614 (1972).
[56] J. Araminowicz and J. Dresler, Progress Report No. INR 1464, Institute Badan Jadrowych, Warsaw, Poland, 1973, p. 14.
[57] K. Sailer, S. Daroczi, P. Raics, and S. Nagy, in ''Proceedings of the Conference on Neutron Physics,'' Kiev, USSR, 1977, Report No. INDC(CCP)-118/G, 1977, p. 246.
[58] N. I. Molla, M. M. Islam, M. M. Rahman, and S. Khatun, Progress Report No. INDC(BAN)-002, IAEA, Vienna, Austria, 1983.
[59] M. Ibn Majah and A. A. Haddun, Report No. INDC(MOR)-003/GI, Vienna, Austria, 1984.
[60] B. M. Bahal and R. Pepelnik, Report GKSS 84/E, Forschungszentrum Geesthacht GmbH, Geesthacht, Germany, 1984.
[61] I. Ribansky, T. Pantaleev, and L. Stoeva, Ann. Nucl. Energy **12**, 577 (1985).
[62] D. L. Smith, J. W. Meadows, and F. F. Porta, Nucl. Sci. Eng. **78**, 420 (1981).
[63] S. M. Qaim, Nucl. Phys. **A382**, 255 (1982).
[64] T. Kobayashi, A. Taniguchi, T. Ikuta, K. Kawade, H. Yamamoto, T. Katoh, T. Iida, and A. Takahashi, in ''Proceedings of the 1990 Symposium on Nucl. Data,'' edited by M. Igashira and T. Nakagawa, Report No. JAERI-M 91-032, NEANDC(J)-160/U, INDC(JPN)-148/L, JAERI, Tokei-mura, Naka-gun, Ibaraki-ken, Japan, 1991.
[65] S. M. Qaim, in *Neutron Cross Section Curves*, *Neutron Cross Sections* Vol. 2, edited by V. McLane, C. L. Dunford and P. F. Rose (Academic Press, New York, 1988).
[66] Hoang Dac Luc, in *Neutron Cross Section Curves*, *Neutron Cross Sections* Vol. 2, [65].
[67] A. Fessler and S. M. Qaim, Radiochim. Acta (submitted).
[68] N. I. Molla, R. U. Miah, S. Basumia, S. M. Hossain, and M. Rahman, in *Proceedings of the International Conference on Nuclear Data for Science and Technology*, Trieste, 1997, edited by G. Reffo, A. Ventura, and C. Grandi (Italian Physical Society, Bologna, Italy, 1997), p. 517.